To cite this version :

Achraf FERSI, AYED YESSINE, LAVISSE BRUNO, Guenael GERMAIN - Identification of friction coefficient between uncoated carbide tool and Ti-6Al-4V alloy under different lubrication conditions - In: ESAFORM, France, 2024-04-24 - Materials Research Proceedings - 2024

Identification of friction coefficient between uncoated carbide tool and Ti-6Al-4V alloy under different lubrication conditions

FERSI Achraf[1,a*], AYED Yessine[1,b], LAVISSE Bruno[1,c] and GERMAIN Guénaël[1,d]

[1]Arts et Metiers Institute of Technology, LAMPA, HESAM Universite, F-49035, Angers, France

[a]achraf.fersi@ensam.eu, [b]yessine.ayed@ensam.eu, [c]bruno.lavisse@ensam.eu,
[d]guenael.germain@ensam.eu

Keywords: Friction Coefficient, Cryogenic Condition, Titanium Alloy, Adhesion, Numerical Simulation

Abstract. During machining, the friction between the tool and the workpiece (cutting face and flank face) is a significant tribological phenomenon because it strongly influences the cutting operation. Indeed, higher friction leads to an increase of cutting forces, a greater heat generation, a premature tool wear and a surface degradation. This study focuses on tool (WC/Co)/workpiece (Ti-6Al-4V) friction under different cooling conditions (dry, emulsion, cryogenic). Determining the friction coefficient requires numerical simulations to separate the tribological phenomena. For this purpose, several modeling methods are compared (Lagrangian, CEL, and ALE). Experimental tests revealed that the friction coefficient depends not only on the sliding velocity but also on lubrication modes. Specifically, the lowest friction coefficient is obtained under cryogenic condition. Adhesive phenomena on the WC/Co pin are observed in the friction zone, particularly at high sliding velocities.

Introduction

Titanium alloys have garnered significant attention from both industries and researchers due to their remarkable mechanical properties. These properties include good fatigue strength, corrosion resistance and a high strength-to-weight ratio, even at elevated temperatures. Titanium alloys find widespread use in various sectors, including aeronautics, automobile production, and the medical industry. However, machining titanium alloys is a challenging task. They are considered as difficult-to-cut materials. During the cutting process, their low thermal conductivity and high chemical reactivity with tool materials lead to accelerate tool wear. The friction generated at the interfaces between the cutting tool and the workpiece or/and chip significantly influences tool wear, ultimately impacting tool life.

Numerous studies, such as those carried out by [1-3], have investigated the tribological behavior during machining. In particular, [4] characterized friction between Ti-6Al-4V alloy and WC/Co. Surprisingly, they found that the friction coefficient remained unchanged for dry contact, as well as under both liquid nitrogen and gaseous nitrogen conditions. Interestingly, the results from [5] revealed that the presence of liquid carbon dioxide (LCO2) during tribology tests led to an increase in the friction coefficient. However, when combined with oil (LCO2+oil), the friction coefficient decreased by a substantial 80%. Researchers have emphasized that not only the choice of cutting tool and workpiece materials affects the friction coefficient [6], but also the nature of the machining process [7] and the cooling/lubrication conditions [8].

The current study aims to investigate the effect of sliding speed and friction conditions (including dry, emulsion, and cryogenic environments) on the tribological behavior of Ti-6Al-4V alloy when using carbide tools. The apparent friction coefficient will be determined under different lubrication conditions and conduct a numerical study to identify the adhesive friction coefficient.

Tribometer device and test procedure

Friction tests were conducted using an open tribometer, as depicted in Figure 1. The design of this tribometer was inspired from the work of reference [9]. The fundamental principle underlying this device involves the application of a normal force through a spherical-tipped pin made of the same material as the cutting tool (tungsten carbide). The pin presses against a rotating Ti-6Al-4V workpiece maintained in the chuck of a Leadwell CNC LTC25iL lathe. As it moves along the X-axis of the lathe, the pin's trajectory forms a spiral. The tribometer is considered "open" because the pin does not rub against an already worn surface. A rigid spring applies the normal force (F_N). The resulting apparent friction coefficient (μ_{app}) is calculated as the ratio between the tangential and normal forces:

$$\mu_{app} = \frac{F_T}{F_N} \tag{1}$$

F_N is the normal force and F_T is the tangential force. They were measured using a Kistler dynamometer (9257B). The tribometer provides macroscopic data that incorporates two phenomena: the adhesion phenomenon and the plastic deformation generated under the pressure of the pin on the material surface. The apparent friction coefficient does not therefore represent the real friction coefficient. Indeed, the real coefficient of friction is due exclusively to the adhesion phenomenon. Bowden and Tabor [10] proposed a decomposition of the apparent friction coefficient (μ_{app}) in two parts as:

$$\mu_{app} = \frac{F_T}{F_N} = \mu_{adh} + \mu_{plast-def} \tag{2}$$

With μ_{adh} is the adhesive friction coefficient (or real coefficient of friction) and $\mu_{plast-def}$ is the plastic deformation coefficient. The determination of the adhesive friction coefficient μ_{adh} is not possible through experimental tests, it must be calculated by subtracting $\mu_{plast-def}$ from the measured μ_{app} coefficient. Therefore, it's necessary to simulate the friction test numerically to decorrelate the two phenomena, and identify the adhesive coefficient μ_{adh} using an inverse approach.
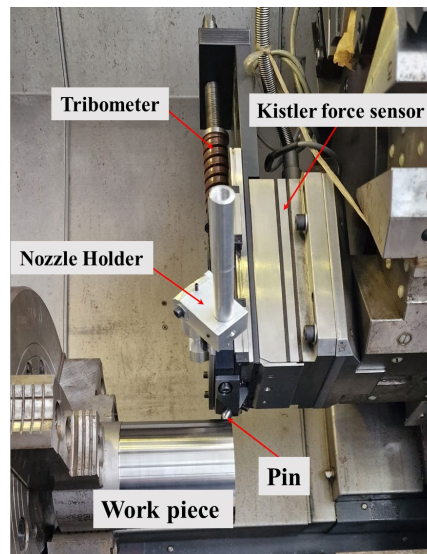

Fig. 1: Experimental setup

Testing conditions

According to the results of [11] and [12], it has been proved that the contact pressure in the cutting zone during the machining of titanium alloy Ti-6Al-4V using carbide tools reaches a value of 1.5 GPa. The magnitude of the normal force (F_N) required to maintain this contact pressure level at the pin/workpiece interface, was estimated by numerical simulation. The calculated value is 350 N. Table 1 presents the selected friction conditions. V_g represents the sliding speed between the pin and the workpiece.

Table 1: friction conditions

Vg (m/min)	F_N (N)
15	
30	350
45	
60	
75	
90	

Numerical simulation

Model presentation

To simulate the friction test, ABAQUS/Explicit FEM solver is used. The pin is modeled by a spherical tip (Ø 9 mm) and an upper rigid part. It is meshed using C3D4 tetrahedral elements of a size of 400 µm. A reference point (RP) located on the rigid zone permits to manage its displacement. The workpiece is modeled with a parallelepiped form, and it is meshed using C3D8R hexagonal elements. The mesh size in the contact zone is around 50 µm. Mesh size and type are selected based on literature review (e.g. [9], [14], and [15]) and on a sensitivity study of results to mesh parameters. The model geometry is presented by Fig.2. The mechanical properties of the work material and the pin are reported in table 2.
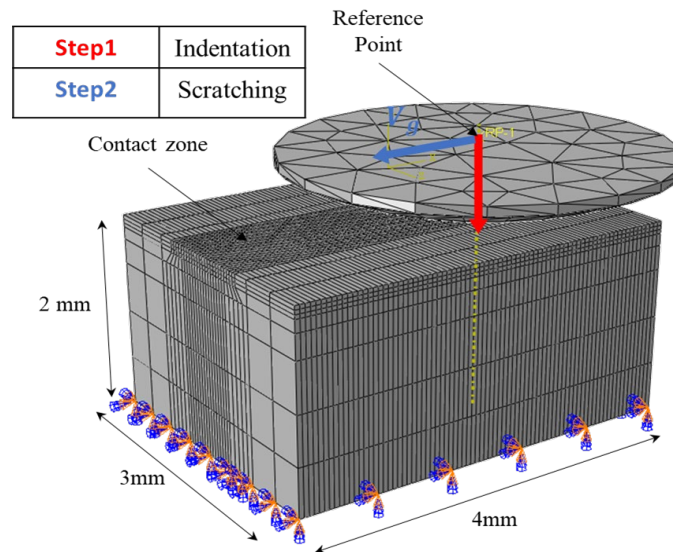

Fig.2: Geometry of the model

The simulation is carried out in two steps: (i) an indentation step and (ii) a scratching step. First of all, during the indentation step, the pin moves vertically as it indents the material, to reach the

penetration depth (h) required to maintain the targeted contact pressure. Then, during the scratching step, the pin moves horizontally rubbing on the contact surface with the sliding speed (V_g). The workpiece is fixed via the nodes of the bottom surface (Fig.2).

Table 2 : Mechanical properties of materials [13]

Properties	WC	Ti-6Al-4V
Density ρ ($Kg\,m^{-3}$)	12800	4420
Young's modulus E (Gpa)	630	114.5
Poisson's ratio v	0.22	0.31
Specific heat C_p (J $Kg^{-1}C^{-1}$)	226	580
Heat conductivity λ (W$C^{\circ -1}m^{-1}$)	44.6	6.6

The Johnson-Cook plasticity model is used to describe the mechanical behavior of the Ti-6Al-4V (equation 3). It is based on the Von Mises yield criterion and it considers the effect of strain hardening, strain rate and temperature. The model parameters are reported in table 3:

$$\bar{\sigma} = \left(A + B \cdot \bar{\varepsilon}_p^n\right).\left[1 + C.\,\text{Ln}\left(\frac{\dot{\varepsilon}_p}{\dot{\varepsilon}_{p0}}\right)\right].\left[1 - \left(\frac{T - T_{amb}}{T_{fus} - T_{amb}}\right)^m\right] \tag{3}$$

Table 3: Johnson-Cook parameters of Ti-6Al-4V [13]

A (MPa)	B (MPa)	n	m	T_{fus} (°C)	T_{amb} (°C)
800	743	0,3	0,7	1655	20

Contact modelling

The contact between the pin and the workpiece is modeled by Coulomb friction law as follows:

$$\tau_f = \mu_{adh}\sigma_n \tag{4}$$

With τ_f is the tangential stress, σ_n is the normal stress and μ_{adh} is the adhesive friction coefficient.

Numerical modeling strategies

According to the literature (e.g. [9], [14] and [15]) three distinct approaches could be used to simulate the friction test: (i) Lagrangian approach, (ii) CEL (Coupled Eulerian-Lagrangian) approach and (iii) ALE approach (Arbitrary Eulerian-Lagrangian) approach. In the present work, these different strategies have been deployed and tested. Their performance has been evaluated in terms of results, accuracy and computation time.

For this study, to determine the best modeling strategies, the models have the same configurations. The adhesive friction coefficient μ_{adh} introduced into the model to characterize the mechanical contact, was maintained at 0.1. The sliding speed (V_g) was fixed at 50 m/min.

Numerical results

For each simulation, the normal and tangential forces (F_N and F_T) were recovered as shown in Fig.3. The apparent numerical friction coefficient is calculated according to equation (1).
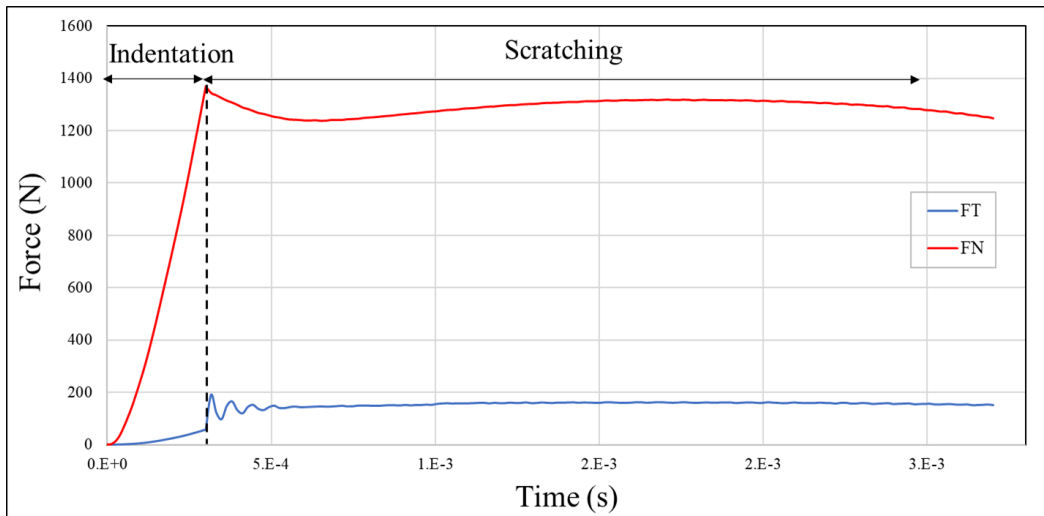
Fig. 3: Evolution of numerical forces; Lagrangian model

Table 5 highlights the results obtained for each modeling strategy. Although the difference in the friction coefficient is less than 3%, the computation time varies considerably. In fact, the "Lagrangian" model is 6 times faster than the "CEL" model, and it is 14 times faster than the "ALE" model. This substantial difference in computation time is an important factor to consider when choosing the appropriate model for a given analysis. The results show that Lagrangian model is the best choice. This model is used in the rest of the study to calculate the coefficient of friction.

Table 4: Simulation parameters

	Parameters		CEL	ALE	Lagrangian
Workpiece	Element size (µm)	Local	50	50	50
		Global	500	500	500
	Type		EC3D8R	C3D8R	C3D8R
	Number		14 400	19 200	19 200
Pin	Element size (µm)		400	400	400
	Type		C3D4	C3D4	C3D4
	Number		819	819	819
Rigid part	Size (µm)		600	600	600
	Type		C3D4	C3D4	C3D4
	Number		230	230	230

Table 5: Friction coefficients

Model	Apparent friction coefficient	Computing time
Lagrangian	0.122	2h and 15 min
CEL	0.125	14h
ALE	0.127	33h

Adhesive friction coefficient

The determination of the adhesive friction coefficient μ_{adh} proceeds through several successive steps. Initially, experimental friction tests were conducted to determine the apparent friction

coefficient ($\mu_{app-exp}$). Then, numerical simulations were performed to reach the same experimental normal force ($F_{N\_num} = F_{N\_exp}$ = 350 N). Finally, numerical simulations were conducted to obtain a numerical friction coefficient similar to the experimental friction coefficient by adjusting the adhesive friction coefficient μ_{adh} introduced in Abaqus ($\mu_{app-num} = \mu_{app-exp}$). The sliding velocities (Vg) are the same values as tested during the experimental approach (table 1).

To separate the two parts of the apparent friction coefficient mentioned in equation (2) and identify the adhesive friction coefficient μ_{adh}, one simply subtracts the adhesive friction coefficient (μ_{adh}) from the numerical friction coefficient ($\mu_{app-num}$).

Fig.4 presents the proportions of the adhesive friction coefficient and the plastic deformation for each sliding speed, it appears that adhesive friction coefficient μ_{adh} comprises over 95% of the apparent friction, irrespective of the sliding speed. Consequently, the apparent friction coefficient measured with the tribometer corresponds mainly to the adhesive friction coefficient. As a result, throughout the rest of the study, only the apparent coefficient of friction will be considered.
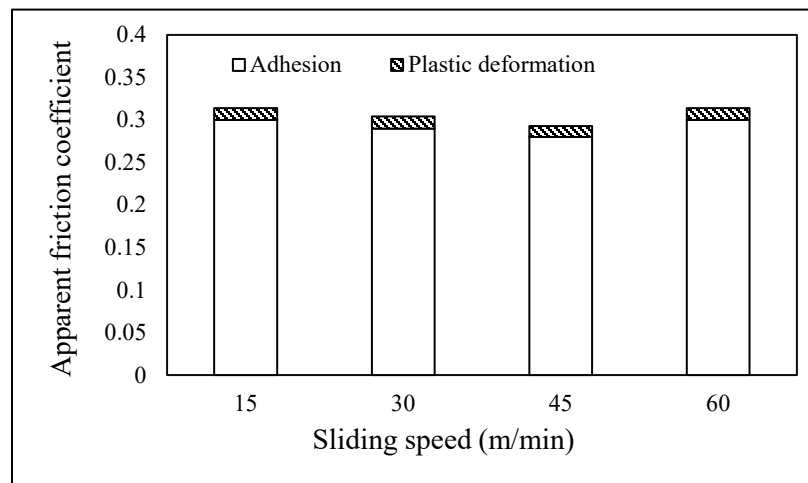

Fig.4 : Proportion of adhesion and plastic deformation; dry friction

Experimental tests conditions
The friction tests were conducted under two lubrication conditions:
- **Cryogenic assistance:** A nozzle with a 2 mm diameter is used to project liquid nitrogen (LN2) onto the contact zone (pin/workpiece) with a flow rate of 2.95 L/min and under a pressure of 12 bar.
- **Emulsion:** A cutting fluid (ECOCOOL CS+) with a 6% oil concentration in the emulsion is projected onto the pin/workpiece interface using a nozzle of 8 mm diameter and under a pressure of 20 bar.

Results and discussion
Fig.5 illustrates the evolution of experimental apparent friction coefficient versus the sliding speed for the three friction conditions. The results clearly demonstrate that the experimental apparent friction coefficient ($\mu_{app-exp}$) varies as the sliding speed increases. The friction coefficient exhibits similar trends across all tested conditions, revealing two behaviors. Below a sliding speed of 45 m/min, the friction coefficient decreases until it reaches a minimum value. Conversely, at sliding speeds from 45 m/min to 90 m/min, the friction coefficient starts to increase.
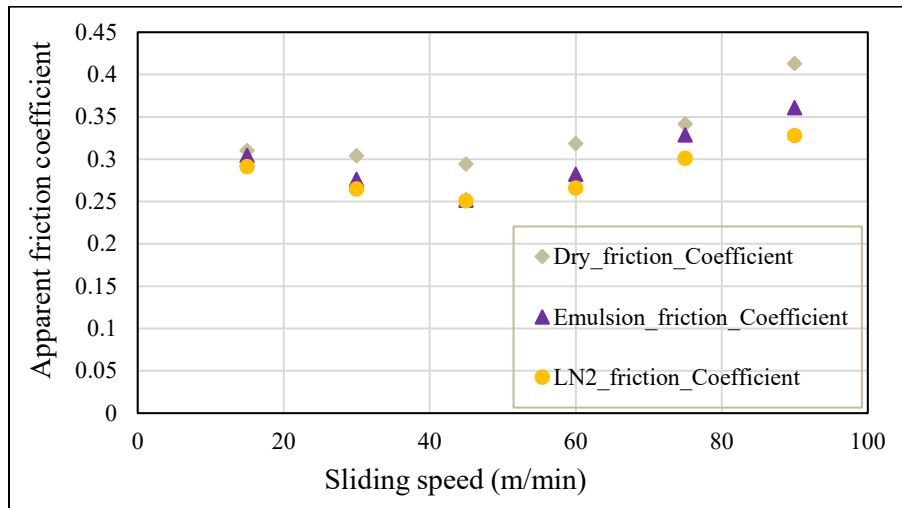
Fig.5: Evolution of friction coefficient in function of the sliding speed, under different lubrication conditions

These results are in line with the works of [16] and [17] concerning the evolution of the friction coefficient in function of the sliding speed.

The introduction of a lubricating fluid influences the tribological behavior of the pin/workpiece interface. Indeed, the fluid forms a film that modifies the temperature and the properties of this interface. These results are consistent with those of the study [16], which reported that lubrication using ester oil, resulted in a lower friction coefficient than dry friction.

The authors of the study [17] noted that the friction coefficient decreased under the effect of liquid nitrogen (LN2) compared to dry friction. However, contradictory results were reported by the authors of studies [4] and [8], who concluded that cryogenic assistance methods with LN2, LCO2, or LCO2+MQL had no effect on the friction coefficient.

Figure 6 illustrates a chemical analysis conducted via Energy-Dispersive X-ray Spectroscopy (EDS) of the pin surface. The results show that titanium which adhered to pin surface is affected by both the lubrication fluid nature and the sliding velocity. The EDS analysis are consistent with the results of [16], which reported that the cryogenic bath limited efficiently the occurrence of adhesion. Similarly, the authors of the study [18] indicated that the introduction of lubrication fluid or Minimum Quantity Lubrication (MQL) reduced the contact area by 35 % compared to dry friction. These studies confirm that the choice of lubrication configuration restricts the phenomenon of adhesion compared to dry friction.
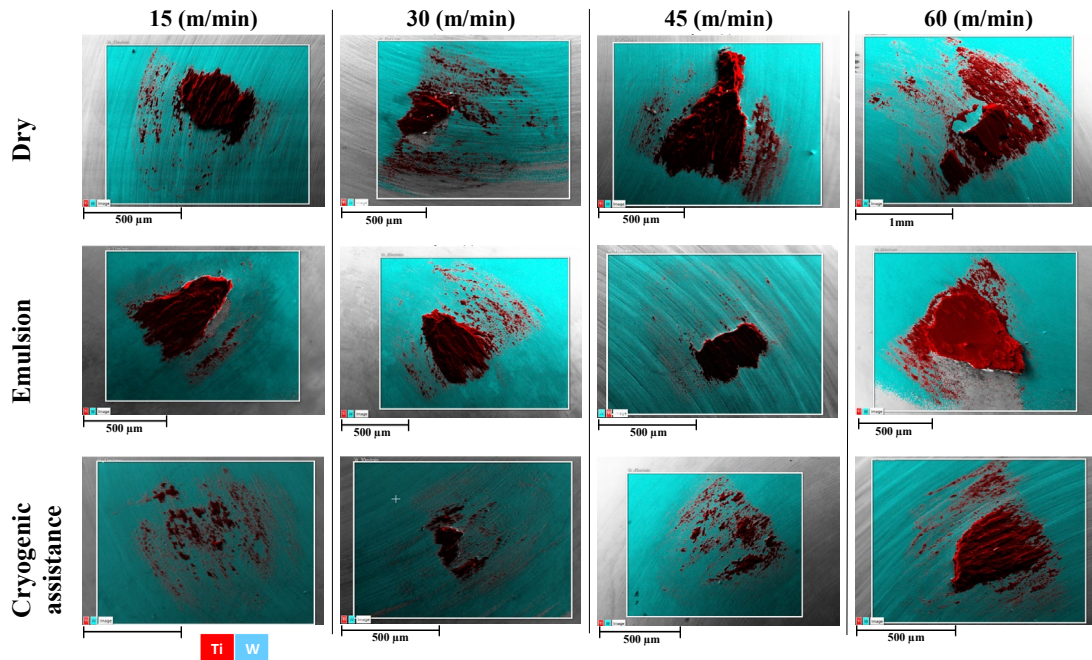
Fig.6: EDS analysis

According to the previous results, the extreme contact conditions (high pressure and temperature) resulted in the phenomenon of adhesion. Figure 6 shows that adhesion zones are relatively similar for sliding speeds between 15 and 45 m/min. However, the size of adhesion zone increases significantly at higher sliding speed. This is more pronounced for the cryogenic configuration. These results are consistent with those of previous researches such as [4] and [19]. The high temperature in the contact zone leads to rise the temperature of the deformed region of the material, resulting in a change of its mechanical properties. The adhered layer of titanium transformed the nature of contact from carbide/titanium to titanium/titanium. The shearing between the adhered titanium and the titanium of the work material increases the tangential forces, resulting in an increase in the friction coefficient. The presence of a lubrication fluid has a notable impact on the tool/workpiece interface behavior by reducing the friction coefficient. Additionally, the injection of liquid nitrogen into the contact zone leads to restrict the adhesion phenomena. Consequently, the shear forces between the adhered portion and the workpiece decrease, resulting in a reduction of the friction coefficient, of the order of 5 % compared to emulsion and 12 % compared to dry machining.

Conclusion

This study investigated the frictional behavior of Ti-6Al-4V using tungsten carbide tools under different conditions: dry, lubricated, and cryogenic (LN2). Numerical modeling was employed to determine the coefficient of adherent friction (real friction coefficient). The tests were conducted at sliding speeds ranging from 15 m/min to 90 m/min, with a force of 350 N, corresponding to an estimated contact pressure of 1.5 GPa. Under these frictional conditions, titanium exhibits strong adhesion, significantly impacting the contact behavior. The results highlighted the influence of varying sliding speed on the friction coefficient. In the emulsion condition the friction coefficient is reduced by 5% compared to dry condition. It is further reduced by 12% under cryogenic cooling.

References

[1] M. Bogdan-Chudy et al., « Tribological and thermal behavior with wear identification in contact interaction of the Ti6Al4V-sintered carbide with AlTiN coatings pair », Tribol. Int., vol. 167, p. 107394, mars 2022. https://doi.org/10.1016/j.triboint.2021.107394

[2] N. Uçak, J. Outeiro, K. Aslantas, A. Çiçek, et B. Çetin, « Determination of the friction coefficients between uncoated WC-Co tools and L-PBF and wrought Ti-6Al-4V alloys for micro-milling simulations », Procedia CIRP, vol. 117, p. 281-286, 2023. https://doi.org/10.1016/j.procir.2023.03.048

[3] S. Basten, L. Seis, M. Oehler, B. Kirsch, H. Hasse, et J. C. Aurich, « Tribological behaviour of AISI 4140 and WC-Co carbides during dry condition, using cryogenic media, and sub-zero metalworking fluids at high contact stresses », Wear, vol. 512-513, p. 204525, janv. 2023. https://doi.org/10.1016/j.wear.2022.204525

[4] C. Courbon, F. Pusavec, F. Dumont, J. Rech, et J. Kopac, « Tribological behaviour of Ti6Al4V and Inconel718 under dry and cryogenic conditions—Application to the context of machining with carbide tools », Tribol. Int., vol. 66, p. 72-82, oct. 2013. https://doi.org/10.1016/j.triboint.2013.04.010

[5] F. Pušavec, L. Sterle, M. Kalin, D. Mallipeddi, et P. Krajnik, « Tribology of solid-lubricated liquid carbon dioxide assisted machining », CIRP Ann., vol. 69, no 1, p. 69-72, 2020. https://doi.org/10.1016/j.cirp.2020.04.033

[6] D. Smolenicki, J. Boos, F. Kuster, H. Roelofs, et C. F. Wyen, « In-process measurement of friction coefficient in orthogonal cutting », CIRP Ann., vol. 63, no 1, p. 97-100, 2014. https://doi.org/10.1016/j.cirp.2014.03.083

[7] C. Bonnet, J. Rech, et G. Poulachon, « Characterization of friction coefficient for simulating drilling contact for titanium TiAl6V4 alloy », CIRP J. Manuf. Sci. Technol., vol. 29, p. 130-137, mai 2020. https://doi.org/10.1016/j.cirpj.2020.03.003

[8] C. Courbon, L. Sterle, M. Cici, et F. Pusavec, « Tribological Effect of Lubricated Liquid Carbon Dioxide on TiAl6V4 and AISI1045 under Extreme Contact Conditions », Procedia Manuf., vol. 47, p. 511-516, 2020. https://doi.org/10.1016/j.promfg.2020.04.139

[9] F. Zemzemi, J. Rech, W. Ben Salem, A. Dogui, et P. Kapsa, « Identification of a friction model at tool/chip/workpiece interfaces in dry machining of AISI4142 treated steels », J. Mater. Process. Technol., vol. 209, no 8, p. 3978-3990, avr. 2009. https://doi.org/10.1016/j.jmatprotec.2008.09.019

[10] F. P. Bowden et D. Tabor, The Friction and Lubrication of Solids. Clarendon Press, 2001.

[11] M. Sima et T. Özel, « Modified material constitutive models for serrated chip formation simulations and experimental validation in machining of titanium alloy Ti–6Al–4V », Int. J. Mach. Tools Manuf., vol. 50, no 11, p. 943-960, nov. 2010. https://doi.org/10.1016/j.ijmachtools.2010.08.004

[12] Y. Karpat, « Temperature dependent flow softening of titanium alloy Ti6Al4V: An investigation using finite element simulation of machining », J. Mater. Process. Technol., vol. 211, no 4, p. 737-749, avr. 2011. https://doi.org/10.1016/j.jmatprotec.2010.12.008

[13] C. Ramirez, « Critères d'optimisation des alliages de TITane pouraméliorer leur USinabilité », p. 253, 2009.

[14] H. Ben Abdelali, C. Claudin, J. Rech, W. Ben Salem, Ph. Kapsa, et A. Dogui, « Experimental characterization of friction coefficient at the tool–chip–workpiece interface during dry cutting of AISI 1045 », Wear, vol. 286-287, p. 108-115, mai 2012. https://doi.org/10.1016/j.wear.2011.05.030

[15] N. Fezai et al., « Characterization of friction for the simulation of multi-pass orthogonal micro-cutting of 316L stainless steel », Procedia CIRP, vol. 108, p. 845-850, 2022. https://doi.org/10.1016/j.procir.2022.03.130

[16] L. Meier, N. Schaal, et K. Wegener, « In-process Measurement of the Coefficient of Friction on Titanium », Procedia CIRP, vol. 58, p. 163-168, 2017. https://doi.org/10.1016/j.procir.2017.03.212

[17] E. M. Skalante, H. Makich, et M. Nouari, « Effect of cryogenic friction conditions on surface quality », Procedia CIRP, vol. 108, p. 675-680, 2022. https://doi.org/10.1016/j.procir.2022.03.105

[18] L. Sterle, F. Pušavec, et M. Kalin, « Determination of friction coefficient in cutting processes: comparison between open and closed tribometers », Procedia CIRP, vol. 82, p. 101-106, 2019. https://doi.org/10.1016/j.procir.2019.04.159

[19] A. Egaña, J. Rech, et P. J. Arrazola, « Characterization of Friction and Heat Partition Coefficients during Machining of a TiAl6V4 Titanium Alloy and a Cemented Carbide », Tribol. Trans., vol. 55, no 5, p. 665-676, sept. 2012. https://doi.org/10.1080/10402004.2012.692007